Atmospheric
Chemistry
and Physics

Supplement of

On what scales can GOSAT flux inversions constrain anomalies in terrestrial ecosystems?

Brendan Byrne et al.

Correspondence to: Brendan Byrne (brendan.k.byrne@jpl.nasa.gov)

S1 Detailed analysis of tropical NEE anomalies and ENSO

We examine the agreement between the $GC_{2 \times 2.5-200\%}$ inversion and the proxies/FLUXCOM in the tropics in more detail. Figure S1 (left column) shows the correlation coefficient for each grid cell between the $GC_{2 \times 2.5-200\%}$ NEE anomalies and the proxy/FLUXCOM anomalies. There are broad positive correlations with the NINO 3.4 index across Central and South America, tropical and southern Africa, and much of the Asia-Pacific. Generally, positive correlations are present between $GC_{2 \times 2.5-200\%}$ and SIF, scPDSI, T_{soil}, and FLUXCOM NEE in the Americas, southern Africa, and the Asia-Pacific. Figure S1 (center column) shows the correlation coefficient between the NINO 3.4 index and the proxies over the tropics. Generally, the proxies show strong correlations with the NINO 3.4 index in many of the same regions for which these proxies show strong correlations with $GC_{2 \times 2.5-200\%}$. This suggests that grid-scale correlations between $GC_{2 \times 2.5-200\%}$ and the proxies may be a reflection of the large-scale anomalies across the tropics and do not necessarily imply that the inversion is able to isolate the spatial footprint of ENSO-driven flux anomalies on smaller scales. Alternatively, it is also possible that the proxies themselves do not correlate well with the true NEE at these scales.

We examine whether $GC_{2 \times 2.5-200\%}$ is able to isolate flux anomalies that are separate from the large-scale tropical signal by comparing NEE anomalies for FLUXCOM NEE and $GC_{2 \times 2.5-200\%}$ as a function of time. First, we aggregate $GC_{2 \times 2.5-200\%}$ IAV and FLUXCOM NEE anomalies to the entire tropics and the following continental-scale regions: the Americas, Africa plus the Middle East, and the Asia-Pacific plus the Indian sub-continent (Fig. 1 of main manuscript). Figure S2 shows $GC_{2 \times 2.5-200\%}$ and FLUXCOM NEE anomalies as a function of time over the entire tropics and the continental-scale regions. We show raw and smoothed (3-month running mean) monthly NEE anomalies as a function of time. Over the entire tropics, FLUXCOM and $GC_{2 \times 2.5-200\%}$ are highly correlated ($R^2 = 0.69$) (which is shown in Fig. 2 of main manuscript). On continental scales, the agreement between FLUXCOM and $GC_{2 \times 2.5-200\%}$ is variable, ranging from $R^2 = 0.08$ for Africa plus the Middle East to $R^2 = 0.61$ for the Americas. All correlations improve after smoothing, suggesting that monthly scale variations are not correctly represented in $GC_{2 \times 2.5-200\%}$, FLUXCOM NEE, or both. We attempt to isolate anomalies specific to each continent by removing the large-scale anomaly across the entire tropics. This is done by subtracting a mean tropical anomaly (scaled to have the same variance as the continental anomaly) from the continental anomaly using the following equation:

$$\mathrm{DIFF}_{\mathrm{continent-tropics}} = \mathrm{ANOM}_{\mathrm{continent}} - \mathrm{ANOM}_{\mathrm{tropics}} \times \frac{STD(\mathrm{ANOM}_{\mathrm{continent}})}{STD(\mathrm{ANOM}_{\mathrm{tropics}})}, \tag{1}$$

where $STD()$ represents standard deviation of monthly anomalies. $\mathrm{DIFF}_{\mathrm{continent-tropics}}$ provides an estimate of anomalies in NEE for a given continent that are not associated with the large-scale ENSO-driven anomalies across the tropics. $\mathrm{DIFF}_{\mathrm{continent-tropics}}$ is shown for each continent in Fig. S2e,h,k. The magnitude of the anomalies are reduced after removing the tropical mean anomalies. Positive correlations are obtained for the Americas ($R^2 = 0.18$), Africa plus the Middle East ($R^2 = 0.07$), and the Asia Pacific and India ($R^2 = 0.30$). These results suggest that $GC_{2 \times 2.5-200\%}$ is partially able to isolate NEE anomalies on continental scales that are separate from the large-scale ENSO-induced variability, and suggests that GOSAT flux inversions can be used to examine continental scale flux anomalies in the tropics. We note, however, that the the agreement in NEE IAV between $GC_{2 \times 2.5-200\%}$ and FLUXCOM is not as strong in Africa and the Middle East.

We also examine the continental-scale anomalies in detail for $OSSE_{JULES-100\%}$, $OSSE_{CT2016-100\%}$, and $OSSE_{CT2016-100\%-IAV}$ in Figure S3, which shows the timeseries of continental scale flux anomalies in the tropics for the OSSEs. The correlation between the OSSEs and true anomalies improves after performing a three month running mean, consistent with the GOSAT inversion results. Strong correlations between the OSSEs and true NEE IAV are obtained after removing the mean tropical signal (using equation 1). These results provide further evidence that GOSAT inversions can largely recover continental scale flux anomalies in the tropics.

S2 Impact of prior IAV on posterior NEE IAV

The presence of prior NEE IAV may degrade the posterior NEE IAV due to the fact that the observations under-constrain NEE IAV, such that the prior NEE IAV strongly influences the spatiotemporal distribution of IAV in the posterior NEE. To investigate this, we examined how closely the posterior NEE IAV resembles the prior NEE IAV. Figure S5 shows the agreement between
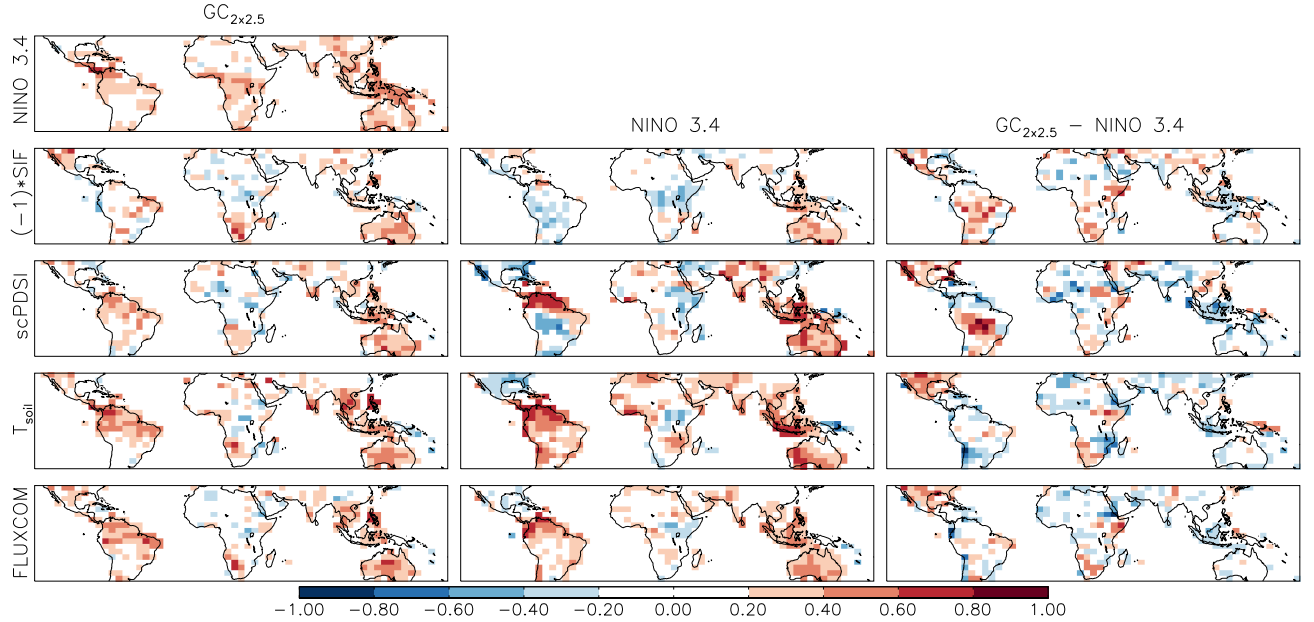
Figure S1. Correlations of monthly anomalies over tropical land at $4° \times 5°$ spatial resolution. Columns show the correlation coefficient (R) of (left) $GC_{2\times2.5-200\%}$ NEE IAV, (center) NINO 3.4 index, and (right) the difference between the two with (top row) the NINO 3.4 index, (second row) $(-1)\times$SIF, (third row) scPDSI, (fourth row) T_{soil}, and (bottom row) FLUXCOM NEE.
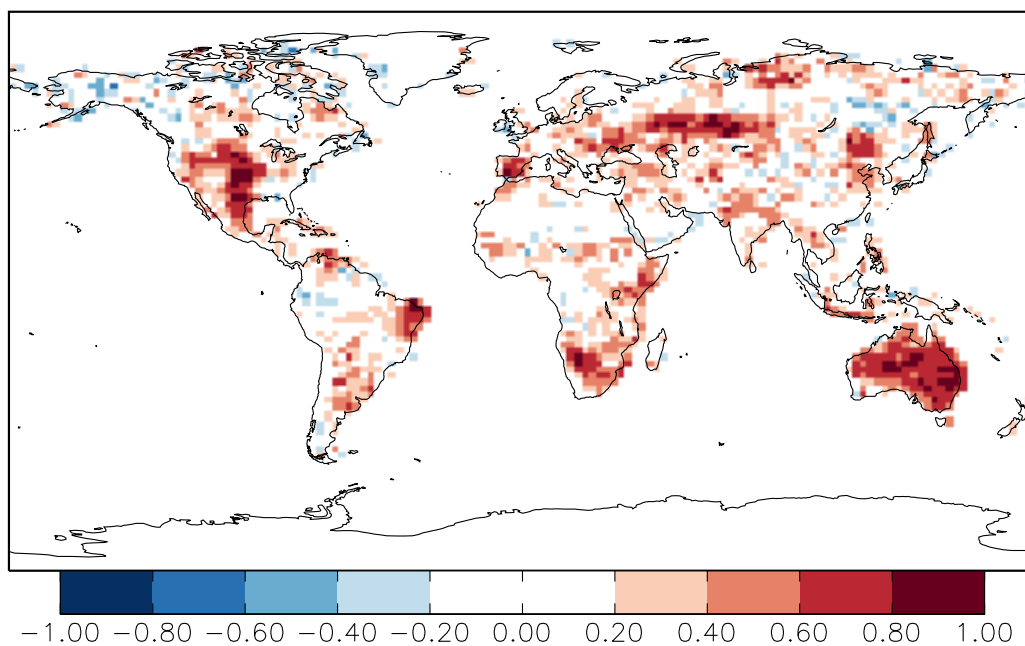
the posterior and prior NEE IAV for $GC_{4x5-100\%-IAV}$ in the tropics and northern extratropics. Posterior NEE IAV is strongly correlated with IAV in the prior NEE, particularly on smaller scales. The fact that correlations between the prior and posterior NEE IAV are strong at $4° \times 5°$ and $8° \times 10°$ is not surprising, as the NEE fluxes are strongly under-constrained at these spatial scales. However, the correlation with the prior NEE IAV is substantially larger than with FLUXCOM on regional ($R^2 = 0.55$ versus $R^2 = 0.15$) and continental ($R^2 = 0.46$ versus $R^2 = 0.26$) scales as well. This suggests that NEE IAV is still under-constrained even on continental scales. Only on the scale of the entire tropics is the correlation with the prior NEE ($R^2 = 0.42$) less than with the proxies ($R^2 = 0.61$ for FLUXCOM NEE and $R^2 = 0.56$ for T_{soil}), indicating that the observations are influencing the posterior NEE IAV more than the prior NEE IAV.
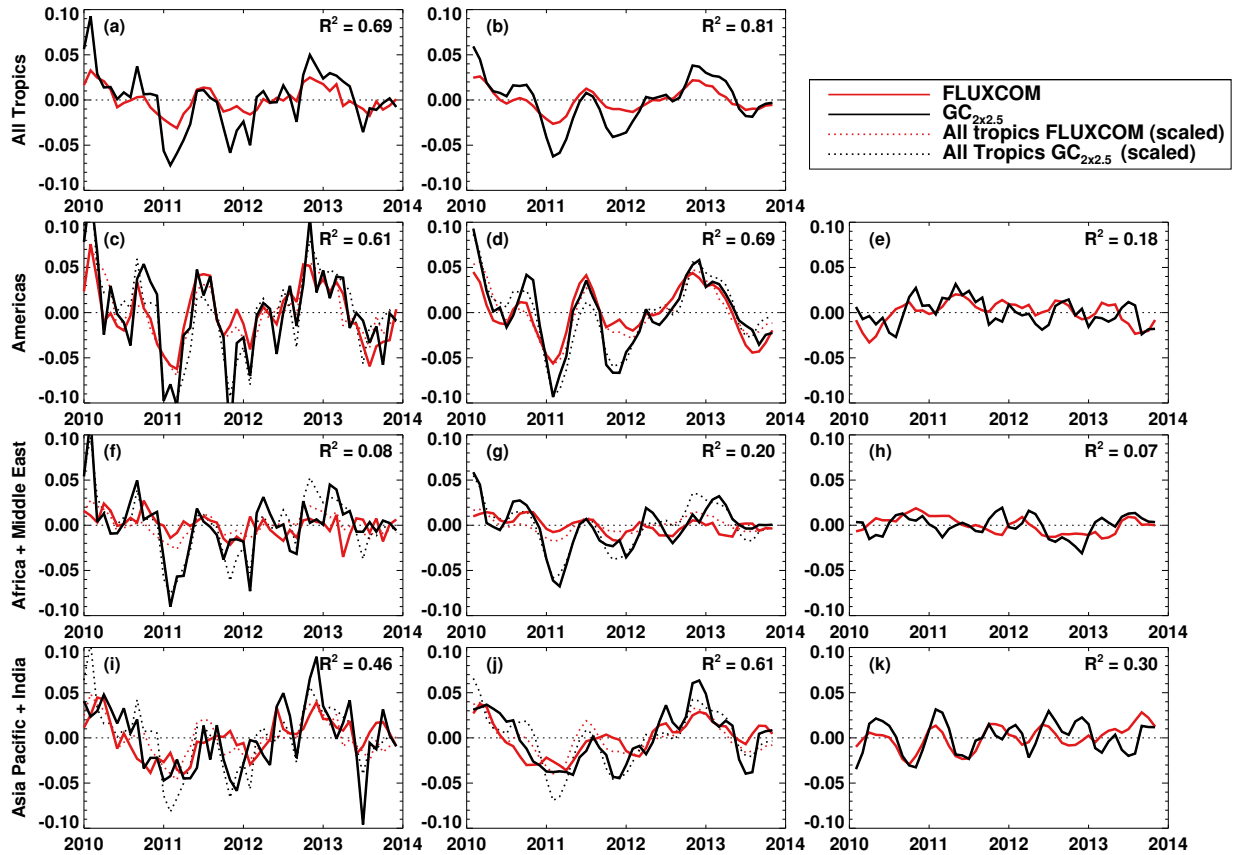
Figure S2. NEE anomalies (gC m^{-2} day^{-1}) for FLUXCOM and GC$_{2\times2.5-200\%}$ in the tropics. (left column) Monthly anomalies, (center column) smoothed (3-month running mean) monthly anomalies, and (right column) DIFF$_{\text{continent}-\text{tropics}}$ (refer to Sect. S1 to see how this is calculated) for (a–b) the entire tropics, (c–e) the Americas, (f–h) Africa and the Middle East, and (i–k) the Asia Pacific and Indian sub-continent. For each sub-plot, R^2 shows the coefficient of determination between GC$_{2\times2.5-200\%}$ and FLUXCOM NEE anomalies within the sub-plot.
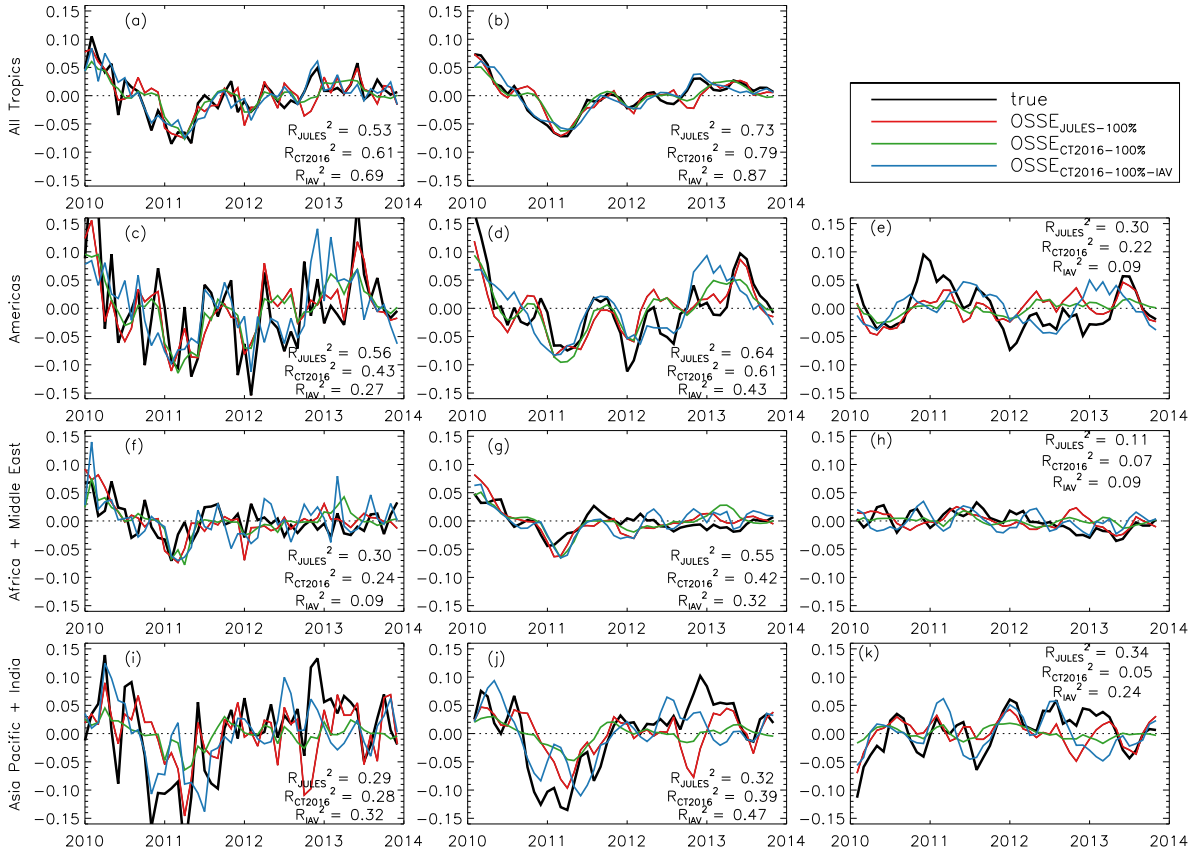
Figure S3. Monthly NEE anomalies (gC m^{-2} day^{-1}) for OSSE$_{\text{JULES}-100\%}$ (red), OSSE$_{\text{CT2016}-100\%}$ (green), OSSE$_{\text{CT2016}-100\%-\text{IAV}}$ (blue) and true NEE IAV (black) in the tropics. (left column) Monthly anomalies, (center column) smoothed (3-month running mean) monthly anomalies, and (right column) DIFF$_{\text{continent}-\text{tropics}}$ (refer to Sect. S1 to see how this is calculated) for (a–b) the entire tropics, (c–e) the Americas, (f–h) Africa and the Middle East, and (i–k) the Asia Pacific and Indian sub-continent.

Figure S4. Correlation between FLUXCOM multivariate regression spline (MARS) GPP anomalies and SIF anomalies at $2° \times 2.5°$ spatial resolution.
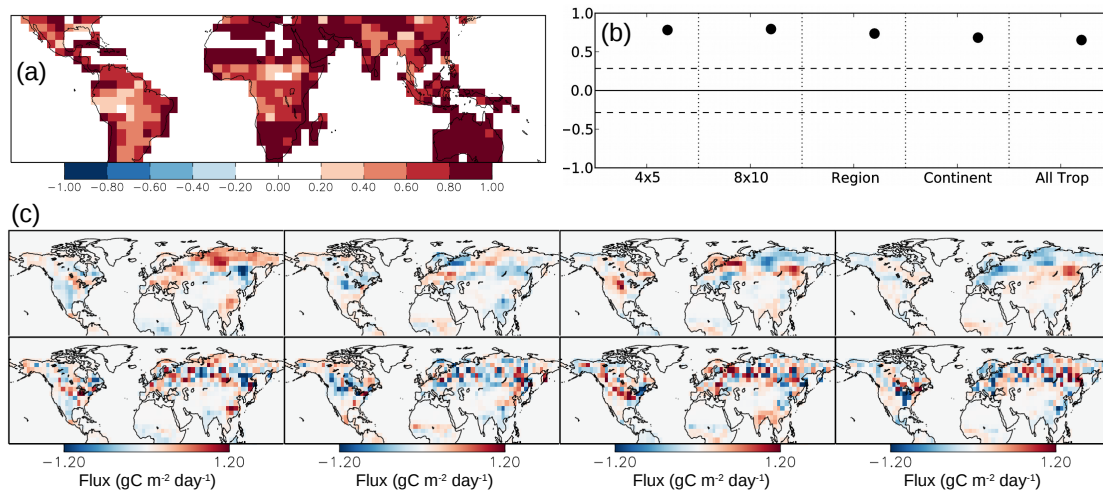
Figure S5. Comparison of GC_{IAV} posterior and prior NEE IAV. (a) Correlation coefficient (R) between the posterior and prior NEE IAV in the tropics at the spatial scale of $4° \times 5°$. (b) Mean correlation coefficient (R) between posterior and prior NEE IAV in the tropics for different degrees of spatial aggregation. (c) Northern extratropical anomalies during JJA for (top) prior and (bottom) posterior NEE for (left–right columns) 2010–2013.